Preparation, Characterization, and Kinetics Model of MoCo/γ-Al_2O_3 Catalysts for Oxidative Desulfurization of Light Naphtha

Beshkoofeh, Sara•; Ghalami Choobar, Bahram*+

Department of Chemistry, University of Guilan, Rasht, I.R. IRAN

Shahidian, Zahra; Khosharay, Shahin

Iranian Institutes of Research and Design in Chemical Industries (IRDCI)-ACECR, Karaj, I.R. IRAN

ABSTRACT: *The subject of this work is to study the effect of pH, molybdenum content, and some of the transition metals (such as Vanadium, Chromium, Manganese, Iron, Cobalt, Nickel) on the catalyst properties and performance of Oxidative DeSulfurization (ODS). To achieve this aim, the mesoporous 5%Co10%Mo/γ-Al_2O_3 catalyst was prepared by the incipient wetness impregnation method. Then, the as-synthesized catalysts were characterized by X-Ray Diffraction (XRD), N_2-adsorption/desorption, Inductively Coupled Plasma Mass Spectrometry (ICP-MS), Scanning Electron Microscopy (SEM) and NH3-Temperature Programmed Desorption (NH_3-TPD). The catalytic activity was measured with a catalytic ODS setup. The catalyst with 10wt%Mo (as an active metal) and 5wt%Co content (as a promoter) at pH=4 represented the optimum performance for oxidative desulfurization. The 5%Co10%Mo/γ-Al_2O_3 has the Surface Area =170.61 m^2/g, Pore Volume =0.64 cm^3/g, and Average Pore Diameter = 15.18nm when these parameters were increased, it led to the best operation condition of sulfur removal. The SEM images showed that the application of Co and Mo metals reaches more homogenous impregnation. The NH_3-TPD result introduced the strong acidic sites of 5%Co10%Mo/γ-Al_2O_3. The obtained results proved that the total sulfur (all kinds of sulfur in the feed) of light naphtha decreased from 160ppm to 20ppm during ODS process with the optimized catalyst. In that case, the kinetics of oxidative desulfurization of the optimized catalyst (5%Co10%Mo/γ-Al_2O_3) was studied. Moreover, a kinetic affinity model was utilized to determine the kinetic parameters of this reaction and the modeling results showed good agreement with experimental data.*

KEYWORDS: *Oxidative desulfurization catalyst; MoCo/γ-Al_2O_3; Light naphtha; Kinetics affinity model.*

***** *To whom correspondence should be addressed.*

+ E-mail: b-ghalami@guilan.ac.ir

● *Other Address Iranian Institutes of Research and Design in Chemical Industries (IRDCI)-ACECR, Karaj, I.R. IRAN:*

*1021-9986/2021/6/1777-1792 16/$/6.0*6

INTRODUCTION

In recent years, the production of transportation fuels has been required. Since sulfur impurities exist in the fuels, they are a major source of air pollution and acid rain. Also, fuels could affect pollution control devices. Therefore, such fuels should be free of polluting compounds and new specifications of sulfur concentration have been established in many different countries [1-9].

The hydrodesulfurization (HDS) process is the current method of reducing sulfur content in diesel fuel. This process is conducted under high pressure, high temperature, and in the presence of Co/Mo or Ni/Mo catalysts. HDS is the most effective process to remove aliphatic sulfur compounds and some derivatives of the thiophene [10,11]. In spite of these advantages, the existing HDS is incapable of meeting ultra-low sulfur standards because of the limited treatment on benzothiophenes (BTs) and dibenzothiophenes (DBTs). It is known that DBTs have alkyl substituents on their 4 or 6 positions [12].

In comparison with HDS method, the Oxidative DeSulfurization (ODS) process is a better choice for reducing sulfur components in diesel. Accordingly, the refractory organic sulfur components are oxidized to their corresponding sulfones. These products can be removed by extraction, adsorption, distillation, or decomposition [13, 14]. In the ODS process, H_2O_2 is commonly utilized as an oxidizing reagent since it is cheap and nonpolluting. Furthermore, it is not a strong corrosive agent and it is commercially available. However, when a catalyst does not exist, H_2O_2 is a weaker oxidizing reagent. Some researchers have described the application of organic acids, and polyoxometallic acids and their salts in the aqueous solution, as catalysts in the oxidation by H_2O_2 of organosulfur compounds to their corresponding sulfones. It is difficult to separate these homogeneous catalysts from the reaction products. However, preparing new supported catalysts of H_2O_2 activation constitutes the most desirable advance in the ODS process [15-17].

Abdullah et al. [18] introduced the MoO_3-PO_4/Al_2O_3 as ODS catalyst, and improved the properties by using alkaline earth metals. The results showed that the activity of the catalyst decreased in the following order: Ca/MoO_3-PO_4/Al_2O_3>Sr/MoO_3-PO_4/Al_2O_3>Ba/MoO_3-PO_4/Al_2O_3. Moreover, the activity of Ca/MoO_3-PO_4/Al_2O_3 catalyst with different Ca/Mo ratios was investigated. When the ratio of Ca/Mo was 15:85, the value sulfur removal was the highest (79%) at 45ºC, 30 min, O/S molar ratio of 3.0, dimetylformamide (DMF) as a solvent, and diesel/solvent ratio of 1.0. *Wenwu et al.* [19] studied the influences of Gallium (Ga) modification on mesoporous Al_2O_3, with emphasis on the changes in the morphology of the active phases and its application as catalyst support for catalytic performances of DBT HDS. The catalyst supports whose wide mesopore size distribution was synthesized from the boehmite sol-gel by using the hydrothermal synthesis approach. Ga_2O_3 was used to modify the synthesized catalyst support. Then the corresponding sulfide NiMo supported catalysts were prepared. The superior catalytic performance was obtained over the NiMoGa/Mo/γ-Al_2O_3 catalyst because of the moderate interaction that exists between the active metals and the supports. The superior morphology for Ni promoted MoS_2 crystals results in the highest degree of sulfidation, the largest proportion of the NiMoS phase, and the enhanced activity of hydrogenation as a result of the introduction of Ga species. Additionally, *Yaseen* [20] reported the promoting influence of Fe as a highly cost-effective and efficient metal and its incorporation to Co or Ni-based MoO_3/Al_2O_3 catalysts in the ODS of DBT in the presence of H_2O_2 and formic acid as an oxidant and a catalyst, respectively. They studied the effect of operating parameters, such as reaction time, reaction temperature, catalyst dose, and amount of oxidant in ODS process. Their results revealed that 99% of DBT conversion was obtained at the temperature of 60ºC and reaction time of 150 min over FeNiMo/γ-Al_2O_3. *Shahidian et al.* [21, 22] prepared a specific type of mesopore extrudates gamma alumina, and they applied it as the catalyst in the heavy oil hydrodesulfurization unit. Using acidic or alkaline treatment, the mesoporous extrudates gamma alumina was made from boehmite powder for the first time. *Morales et al.* [23] modified the CoMo/γ-Al_2O_3 and NiMo/γ-Al_2O_3 which was used in HDS method by using phosphoric acid. *Fattahi et al*. developed some mathematical and kinetic models for catalytic reactor which are used for desulfurization and hydrogenation of oil feed. These models included appropriate kinetic rate expressions of the main hydrogenation reactions [24-29]. In the other investigation, *Garfinkle* [30] used the chemical affinity model for the kinetics of chemical reactions. *Roosta et al.* [31-34] successfully applied the chemical affinity model to the kinetics of gas hydrate formation.

Table 1: Specification the raw materials.

No.	Chemical Name	Initial Mass fraction Purity	Company
1	hydroxyethyl cellulose	Industrial grade	Iran
2	ammonium hepta molybdate tetra hydrate	99%	Merck, Germany
3	phosphoric acid	99%	Merck, Germany
4	ammonia	Industrial grade	Iran
5	nickel (II) nitrate hexahydrate	98%	Applychem, Germany
6	manganese (II) nitrate tetrahydrate	98%	Merck, Germany
7	cobalt (II) nitrate	97%	Merck, Germany
8	chromium (III) nitrate	99%	Merck, Germany
9	Iron (III) nitrate	99%	Merck, Germany
10	*Ammonium* monovanadate	99%	Merck, Germany
11	hydrogen peroxide	Industrial grade	Iran
12	acetonitrile	Industrial grade	Iran

This model requires only the pressures of a consumed mole of the reactants and it does not require mass or heat transfer coefficients. Since this model is simple and applicable, it was chosen as a kinetic model of the present study. *Likozar et al.* [35] used the NiMo catalyst in the hydrotreatment process. It was investigated the mechanism, ab initio calculations, and microkinetics of straight-chain alcohol, ether, ester, aldehyde, and carboxylic acid hydrodeoxygenation over Ni-Mo catalyst.

The present work represents the preparation, characterization, and kinetics affinity model of some of the mesoporous γ-Al_2O_3 catalysts. The different effects are considered, especially for molybdenum content, some transition metals such as Co, Ni, Mn, Cr, Fe, or V and pH. The prepared catalysts are applied to the ODS process of light naphtha with 160ppm sulfur. Moreover**,** the as-synthesized catalysts were characterized by X-Ray Diffraction (XRD), N_2-adsorption/desorption, and Inductively Coupled Plasma Mass Spectrometry (ICP-MS). According to the results of the ODS process and other analyses, the optimized catalyst (5%Co10%Mo/γ-Al_2O_3) was chosen. Then, the properties of 5%Co10%Mo/γ-Al_2O_3 were studied by Scanning Electron Microscopy (SEM) and NH_3-Temperature Programmed Desorption (NH_3-TPD)**.** The chemical affinity model has been applied to several studies on the 5%Co10%Mo/γ-Al_2O_3. The important aspects of this model are explained in the appendix.

EXPERIMENTAL SECTION

Materials

In this research, the boehmite powder, extracted from Azarshahr Nephlinsinite mine ores, was used as the precursor (Surface Area (SA)>200 m^2/g, Pore Volume (PV) =0.48 cm^3/g, Average Pore Diameter (APD) = 8.10 nm, 100mesh). The specification of other raw materials are listed in Table 1.

Characterization

The specific surface area and pore volume of catalysts were measured by using N_2-adsorption/desorption porosimetry (Belsorp mini II, BEL JAPAN). All catalysts were degassed under vacuum at the temperature of 250ºC for 3 h before each measurement (Belprep vac II, BEL JAPAN). This analysis was done in liquid nitrogen at -196ºC. The N_2-adsorption/ desorption isotherms are applied to calculate the Brunauer–Emmett–Teller (BET) specific surface area. Pore volume and pore diameter distribution were computed by using the Barrett–Joyner–Halenda (BJH) technique of the isotherm. The total pore volume was estimated from the N_2 uptake value at P/P_0 = 0.98 (ISO 15901-2-2006, ISO 15901-3-2007). The XRD patterns of the synthesized catalysts were recorded on a Panalytical X' Pert Pro model equipped with a CuKα anti cathode (λ = 1.54 Å; 40kV; 40mA) for 2θ between 5° and 85°. It uses a 0.1° step with an integration time of 4 s. Additionally, ICP-MS was carried out with Perklin Elmer,

Optima 7300 model (U.S.A.). The catalytic oxidative desulfurization activity test is accomplished under the special feed with 160ppm of sulfur and at the ambient condition (35ºC and atmospheric pressure). After this stage, the total sulfur was determined by Rigaku devices (U.S.A.) with a semiconductor Silicone PIN diode detector according to ASTMD: 4294. The surface morphology of the catalysts was conducted by using Scanning Electron Microscopy (SEM) by ZEISS (Germany) SIGMA VP. A study can be carried out with NH_3-TPD analysis and using Micromeritics ChemiSorb 2750 apparatus.

Catalytic Oxidative desulfurization activity

Catalytic experiments were carried out in a 100 mL jacketed round-bottom flask. It was equipped with a condenser, magnetic stirrer, and recirculation water bath to control the temperature at 45ºC and atmospheric pressure. 50 mL of light naphtha (160ppm total sulfur) was used as the oil feed. In a typical run, the prepared catalyst and H_2O_2 were suspended slowly under the vigorous stirring speed in an oil feed (catalyst/oil=0.05 g/mL). After one hour, the mixtures were left at room temperature for one hour. Then the oil phase of samples was withdrawn with acetonitrile three times. The total sulfur was determined by Rigaku devices. The used feed specification (light naphtha) is given in Table 2.

Preparation Method of Oxidative Desulfurization Catalyst and Catalyst Support

The Preparation Extrudates Gamma- Alumina Catalyst Support

Boehmite powder was blended with 5% hydroxylethyl cellulose (HEC). Then adequate water (about 5 mL) was added to it. The mixture was kneaded until a homogeneous paste was obtained. The alumina paste was passed through the extruder and dried for two hours at room temperature. Particularly, it was kept in an oven at 120 ºC for 24hr. Then it was calcined up to 600 ºC by using a furnace with a temperature programming rate of 100 ºC/h for catching the untreated catalyst support. The gamma-alumina phase is formed from the boehmite powder in this section. Appropriately, the catalyst support had the following properties (length=2-7 mm, outer diameter=1.50mm, SA=150-200 m^2/g, PV<0.73 cm^3/g, APD = 13.55 nm).

The Molybdenum Content Effect on Preparation of Mo/γ-Al_2O_3

Mo/γ-Al_2O_3 catalysts were prepared by incipient wetness impregnation method. According to the required weight percent of Mo (0%, 5%, 10%, 15%, and 20%), an appropriate amount of ammonium hepta molybdate was dissolved in a specific volume of distilled water. Each solution with γ-Al_2O_3 catalysts support was placed in the rotary evaporator at 50 ˚C for 2 h. The wet γ-Al_2O_3 was placed in a thermal cabinet with a thermal programming rate of 10 ºC/20 min in the temperature range of (50-120) ˚C. The samples were dried at 120 ˚C for 24hr in an oven. Since stabilization of molybdenum is required to form molybdenum oxide, the catalyst was calcined up to 600 ºC in a furnace with a temperature programing rate of 100 ºC/h.

The pH Effect on Preparation of Mo/γ-Al_2O_3

10%Mo/γ-Al_2O_3 catalysts were selected to study the effect of pH on the decreasing sulfur level. 12.26 g ammonium hepta molybdate was dissolved in 100 mL distilled water at room temperature (25˚C). This ammonium hepta molybdate solution was divided into five portions. Then each pH portion was adjusted between1-5 by using phosphoric acid. Afterwards, each solution with γ-Al_2O_3 catalysts support was placed in the rotary evaporator at 50 ˚C for two hr. Then, the wet γ-Al_2O_3 was placed in a thermal cabinet with the thermal programming rate of 10 ºC/20min (50-120 ˚C). Accordingly, the samples were dried at 120 ˚C for 24 hours in an oven. Similar to the previous section, stabilization of molybdenum is needed to form molybdenum oxide. Therefore, the catalyst was calcined up to 600 ºC in a furnace with temperature programing rate of 100 ºC/h.

The Effect of Transition Metals on Preparation of Mo/γ-Al_2O_3

In this step, some transition metals (such as Vanadium, Chromium, Manganese, Iron, Cobalt, and Nickel) were used as effective metals. They were impregnated on the calcined γ-Al_2O_3 catalyst at pH=4. Firstly, impregnated solution of two salts (solution A and solution B) must be prepared for each catalyst according to Table 2. In order to prepare solutions A and B, each salt must be dissolved in distilled water. Then two solutions (according to Table 3) must be mixed and the pH was stabilized at 4 by using phosphoric acid.

Table 2: Specifications of light naphtha feed.

No.	Analysis	Unit	Result	Method
1	appearance	---	Colorless liquid	Visual
2	Density at 15.6ºC	kg/m^3	736.1	ASTMD1298
3	Total Sulfur	ppm	160	ASTMD4294
4	Flash Point	ºC	free	ASTMD93
5	Corrosion at 50ºC	---	1a	ASTMD130
6	Distillation–IBP	ºC	75	ASTMD86
7	Distillation-5%	ºC	90	ASTMD86
8	Distillation-10%	ºC	95	ASTMD86
9	Distillation-20%	ºC	101	ASTMD86
10	Distillation-30%	ºC	106	ASTMD86
11	Distillation-40%	ºC	111	ASTMD86
12	Distillation-50%	ºC	115	ASTMD86
13	Distillation-60%	ºC	119	ASTMD86
14	Distillation-70%	ºC	125	ASTMD86
15	Distillation-80%	ºC	134	ASTMD86
16	Distillation-90%	ºC	146	ASTMD86
17	Distillation-95%	ºC	162	ASTMD86
18	Distillation-FBP	ºC	192	ASTMD86
19	Distillation- Residue	Vol.%	1	ASTMD86
20	Distillation- Loss	Vol.%	0	ASTMD86
21	Distillation at 380ºC	Vol.%	---	ASTMD86

Table 3: The specification of impregnated solution made with 10 mL of distilled water.

Catalyst	Solution A	Solution B
10%Mo5%V/γ-Al_2O_3	0.63g ammonium hepta molybdate	1.61g *ammonium* monovanadate
10%Mo 5%Cr/γ-Al_2O_3	0.63g ammonium hepta molybdate	1.55g chromium(III) nitrate
5%Mn10%Mo/γ-Al_2O_3	0.63g ammonium hepta molybdate	1.53g Manganese(II) nitrate
10%Mo5%Fe/γ-Al_2O_3	0.63g ammonium hepta molybdate	1.64g iron (III) chloride hexahydrate
10%Mo 5%Co/γ-Al_2O_3	0.63g ammonium hepta molybdate	0.88g cobalt (II) nitrate
10%Mo5%Ni/γ-Al_2O_3	0.63g ammonium hepta molybdate	0.81g nickel (II) nitratehexahydrate

After preparation of each impregnated solution, it was placed in the rotary evaporator at 50℃ for 2 h with γ-Al_2O_3. The wet γ-Al_2O_3 was placed in a thermal cabinet with a thermal program. It was dried in the temperature range of (50-120) ℃. The samples were dried at 120˚C overnight in an oven. Because of stabilizing the molybdenum to form molybdenum oxide, the catalyst was calcined in a furnace with a thermal programmed apparatus at 600 ˚C for 6 h.

Table 4: The BET, BJH results of the prepared catalysts.

Catalyst	BET			BJH (Adsorption branch)		
	Average Pore Diameter (nm)	Surface Area (m^2/g)	Pore Volume (cm^3/g)	Pore Volume (cm^3/g)	Pore Radius (nm)	Surface Area (m^2/g)
0%Mo	13.55	215.43	0.73	0.73	6.03	237.95
5%Mo	14.50	210.83	0.76	0.76	6.03	227.90
10%Mo	15.46	203.97	0.78	0.78	6.03	221.17
15%Mo	13.71	193.67	0.66	0.65	6.03	184.80
20%Mo	13.70	173.20	0.62	0.62	6.03	180.31
10%Mo, pH=1	12.83	177.36	0.56	0.56	6.03	190.70
10%Mo, pH=2	15.46	180.04	0.69	0.69	6.03	193.25
10%Mo, pH=3	15.64	182.75	0.71	0.70	6.03	188.54
10%Mo, pH=4	14.42	190.59	0.68	0.56	6.03	190.70
10%Mo, pH=5	15.34	198.88	0.76	0.76	6.03	213.01
10%Mo5%V/γ-Al_2O_3	15.84	133.35	0.52	0.52	6.91	140.01
10%Mo 5%Cr/γ-Al_2O_3	10.80	162.11	0.43	0.43	6.91	159.91
5%Mn10%Mo/γ-Al_2O_3	15.51	151.46	0.58	0.58	6.03	155.98
10%Mo5%Fe/γ-Al_2O_3	11.49	162.48	0.52	0.52	6.91	173.60
10%Mo 5%Co/γ-Al_2O_3	15.18	170.61	0.64	0.64	6.03	174.98
10%Mo5%Ni/γ-Al_2O_3	14.85	166.87	0.61	0.61	6.23	146.63

RESULTS AND DISCUSSION

Catalyst characterization

Molybdenum content effect

To find the optimum mesoporous catalyst for ODS with H_2O_2, the effect of Mo loading was evaluated. This evaluation is shown in Fig. 1. The catalysts with 0%, 5%, 10%, 15%, and 20%Mo/γ-Al_2O_3 content were prepared and evaluated in catalytic ODS reaction at a feed sulfur concentration of 160 ppm. The obtained result proved that Mo species can be considered as an active metal in the ODS reaction. The conversion of sulfur compounds increases with increasing Mo% content up to 10%. Then the sulfur removal decreases when the percent of Mo is in the range of (10-20) %. As an example, when the catalyst was prepared with 5% Mo, the total sulfur was 120ppm after the ODS process. The catalyst with 10% Mo resulted in 100ppm of total sulfur after the ODS process. When the catalyst with 15% Mo was used, the total sulfur was 117ppm after the ODS process. Using the catalyst with 20% Mo, the total sulfur was 120ppm after the ODS process. Since increasing Mo loading results in more polymerization of Mo species, the activity of the catalyst decreases in the ODS process.

The physicochemical properties and the composition of catalysts are shown in Table 4. The N_2-adsorption/desorption

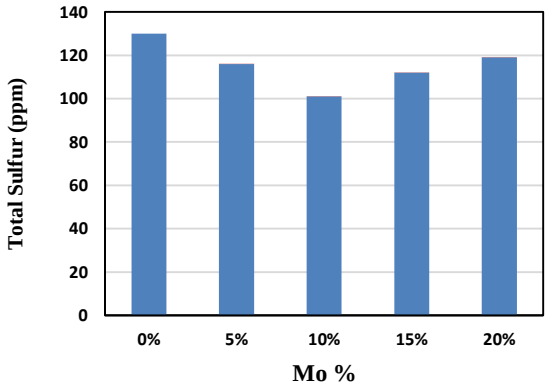

Fig. 1: Catalytic ODS activity test of the different molybdenum content.

results indicated that the Surface Area (SA), Average Pore Diameter (APD) and Pore Volume (PV) of Mo/γ-Al_2O_3 decreased with the increasing the weight percent of Mo which was loaded on the γ-Al_2O_3 catalyst support [19]. It was found that the catalysts with the range of (15-20) Mo% had the lowest sulfur removal in comparison with 0-10Mo %. In the range of (15-20) Mo%, the decrease in SA, PV and MPD resulted in decreasing sulfur removal. Fig. 2 shows up the pore size distribution of the sample measured according to BJH method. It can be seen that the catalyst

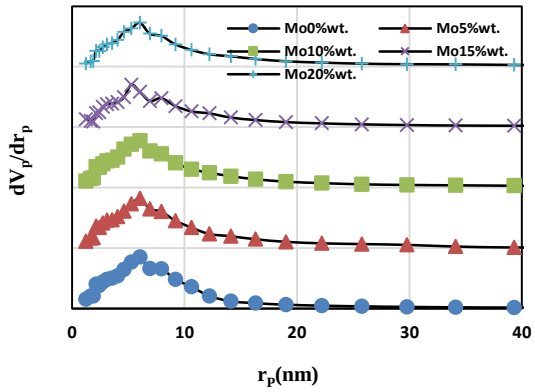

Fig. 2: BJH plot of the different molybdenum content.

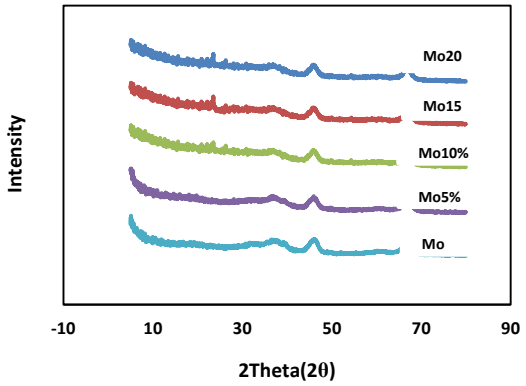

Fig. 4: XRD analysis spectrum of the different molybdenum content.

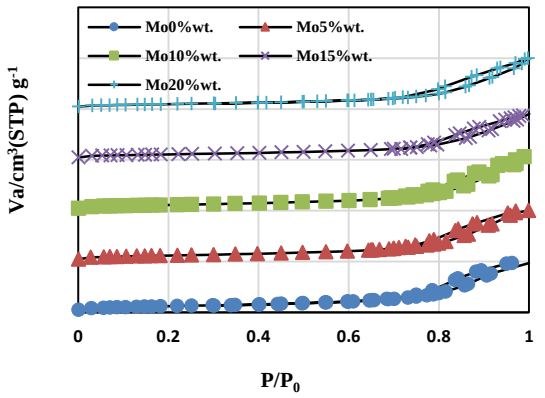

Fig. 3: Adsorption/Desorption isotherms of the different molybdenum content.

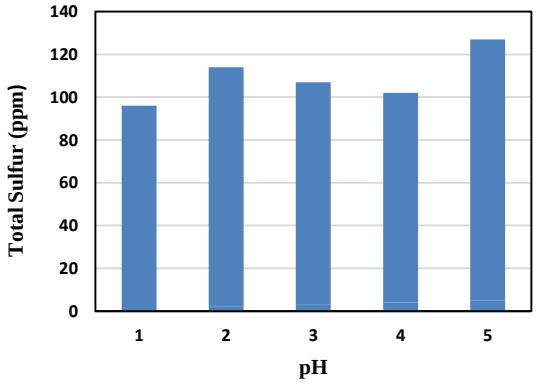

Fig. 5: Catalytic ODS activity test of different pH at 10%Mo/γ- Al_2O_3.

displays a uniform mesoporous structure. According to the IUPAC classification and Fig. 3, all of the prepared mesopore Mo/γ-Al_2O_3 catalysts exhibited type IV isotherms with H_2 hysteresis loop. Typical mesoporous materials due to complex pore networks are made up of pores with wide pore size distribution [19].

Fig. 4 shows the XRD results of catalyst samples with various molybdenum content, including 0wt%, 5wt%, 10wt%, 15wt%, and 20wt%. The results of the tests indicate when the amount of molybdenum is 0wt% and 5wt%, the amorphous phase of MoO_3 is observed on the support. Appropriately, when Mo content increases up to 10wt% MoO_3, 15wt% and 20wt% lead to the formation of the crystalline MoO_3 with broad reflection centering at 2θ (23-27°). These 2θ (23-27°) were attributed to the MoO_3 with orthorhombic phase. In all samples, two specific peaks are observed at 2θ (45 and 67°) related to γ-Al_2O_3. Hence, they are all due to the γ-Al_2O_3 crystalline structure. Accordingly, loading Mo does not affect the γ-Al_2O_3 crystalline structure [36,37]. Therefore, based on the results of ODS, BET, and XRD, the catalyst with 10wt% Mo (PV=0.78 cm^3/g, SA=203.97 m^2/g, APD= 15.46 nm) was selected as the optimum molybdenum concentration.

The pH Effect on Preparation of 10%Mo/γ-Al_2O_3

To find the optimum pH on catalyst activity, all prepared catalysts were tested at different pH values. All experiments were conducted in a catalytic ODS reactor. Fig. 5 displays the results of the catalytic activity of all prepared 10%Mo/γ-Al_2O_3. Consequently, the results reveal that the solution acidity significantly changes the sulfur elimination. Maximum sulfur removal was observed at pH values of 1 and 4. The minimum sulfur removal was perceived at pH=5 [6, 38-40]. The N_2-adsorption/desorption results (Table 4) indicated that the SA and PV of 10%Mo/γ-Al_2O_3 increased with the

Table 5: ICP-MS results of the prepared catalysts.

Catalyst	Al wt.%	P wt.%	Mo wt.%	Other metals wt.%
Mo/γ-Al_2O_3 (pH=1)	54.97	2.33	8.33	-
Mo/γ-Al_2O_3 (pH=2)	55.06	1.16	8.37	-
Mo/γ-Al_2O_3 (pH=3)	55.19	0.58	8.40	-
Mo/γ-Al_2O_3 (pH=4)	55.25	0.22	8.41	-
10%Mo5%V/γ-Al_2O_3	54.85	1.16	8.31	4.01
10%Mo 5%Cr /γ-Al_2O_3	53.41	1.17	8.33	3.17
5%Mn10%Mo/γAl_2O_3	54.93	1.14	8.30	4.40
10%Mo5%Fe/γ- Al_2O_3	54.68	1.17	8.34	3.02
10%Mo 5%Co /γ- Al_2O_3	54.73	1.16	8.36	3.80
10%Mo5%Ni/γ- Al_2O_3	54.80	1.16	8.31	4.02

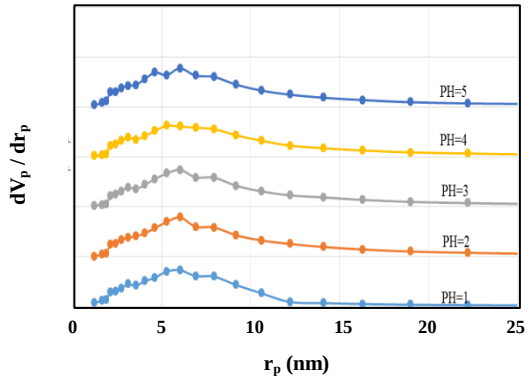

Fig. 6: BJH plot of the different pH at 10%Mo/γ- Al_2O_3t.

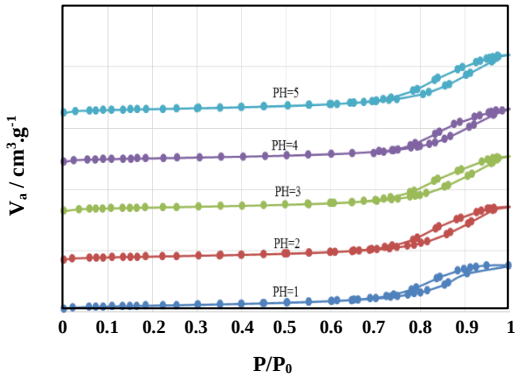

Fig. 7: Adsorption/Desorption isotherms of different pH at 10%Mo/γ- Al_2O_3.

increasing the weight percent of P. The corrosive effect of phosphoric acid, added during impregnation, leads to an increase in SA and PV content. Thus, we could attribute this change in SA and PV either to erosion of the micropores or to blocking of them by the phosphate species [23]. Fig. 6 shows up the pore size distribution of the sample measured according to BJH method. One can see that the catalyst displays a uniform mesoporous structure. According to the IUPAC classification and Fig. 7, all of the prepared mesopore, including 10%Mo/γ-Al_2O_3catalysts at different pH exhibited type IV isotherms with H_2 hysteresis loop [11].

Table 5 shows the results of ICP-MS [41]. The presence of phosphorus is frequently used as a secondary promoter. To improve the performance of the catalyst for ODS, and HDS reactions by possessing beneficial influence on the strength and heat stability of the γ-Al_2O_3. Furthermore, the addition of phosphoric acid during the catalyst preparation reduces the number of required impregnation steps. The enhancing influence of phosphorus on the activity of a catalyst is sometimes explained as a function of improved dispersion of the precursor metal salts on the γ-Al_2O_3. Because of the high solubility of the metal salts on the γ-Al_2O_3 in the phosphoric acid-containing impregnation solution, the deposition of large crystalline aggregates on the γ-Al_2O_3 surface is minimized [41]. Therefore, the catalyst with 10%Mo/γ-Al_2O_3 at pH=4 was selected as an optimum one.

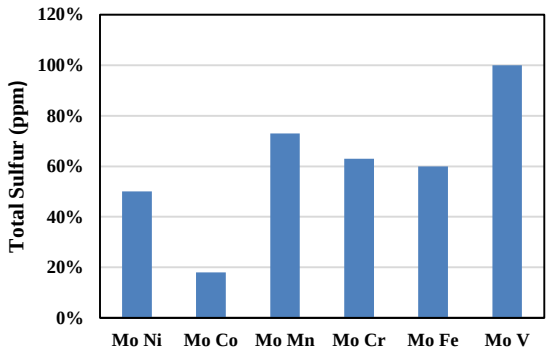

Fig. 8: Catalytic ODS activity test of transition metal.

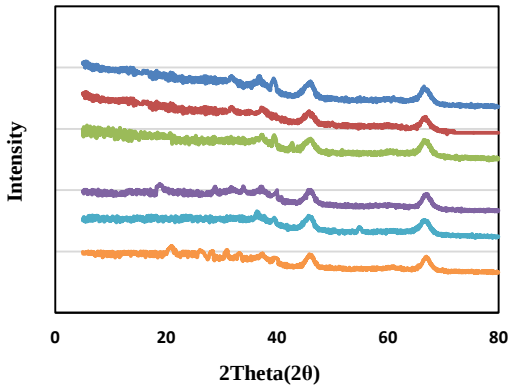

Fig. 9: XRD analysis spectrum of different transition metals.

Effect of transition metals

Some efforts have been done to improve the performance of 10%Mo/γ-Al_2O_3 catalyst by using other transition metals such as Co, Ni, Mn, Cr, Fe, or V in the ODS process. To find the optimum mesoporous catalyst for ODS process, the effect of loading some of the transition metals on 10%MoO_3/γ-Al_2O_3 support at pH=4 was evaluated. The results have been shown in Fig. 8 Furthermore, the catalysts prepared with 10% Mo and 5%Co, 5%Ni, 5%Mn, 5%Cr, 5%Fe, or 5%V with γ-Al_2O_3 as catalyst support. The prepared catalysts were tested in ODS reaction at a feed sulfur concentration of 160 ppm. Fig. 8 shows the conversion of sulfur of the prepared catalysts in the following order: CoMo/γ-Al_2O_3> NiMo/γ-Al_2O_3>FeMo/γ-Al_2O_3>CrMo/γ-Al_2O_3>MnMo/γ-Al_2O_3>VMo/γ-Al_2O_3. Therefore, the 10%Mo5%Co/γ-Al_2O_3 catalyst was selected as the optimum ODS catalyst.

XRD technique was used to get an insight into the chemical composition, crystallinity of catalyst, and presence of Co, Ni, Mn, Cr, Fe, or V in γ-Al_2O_3 supported catalysts. XRD runs were recorded at 2θ (5°- 80°) and the scans are depicted in Fig. 9. Two prominent diffraction peaks that appeared at 2θ (45° and 67°) for all samples are assigned to γ-Al_2O_3. It is concluded that the impregnation of metals did not affect the γ-Al_2O_3 crystalline phase of catalyst support [42]. The results of XRD analysis can be confirmed the fact that almost all metals appeared at their previously reported peaks, Cobalt oxide (Co_3O_4) at 2θ= 32°,36°,37°,45°, and 67° [43], iron oxide (Fe_2O_3) at 2θ= 24°, 33°, 35°,37, 45° and 67° [20], nickel oxide (NiO) at 2θ= 32, 36, 37°, 40, 45° and 67° [44,45], vanadium oxide (V_2O_5) at 2θ= 19°, 26°, 28°, 32°, 33°, 37°,45°, and 67° [46,47], manganese oxide (Mn_2O_3) at 2θ= 17°, 26°, 28°,32°, 33°, 37°, 40°, 45°, and 67° [48], chromium oxide (Cr_2O_3) at 2θ=36°, 37°, 45°,54° and 67° show the characteristic peaks [49,50]. Two peaks exist at 2θ= 45° and 67° for NiO. They are close to specific peaks of γ-Al_2O_3 and they can be assigned to the overlap of defect NiO and γ-Al_2O_3 [43]. For $CoMoO_4$, patterns of the template sample 5%Co10%Mo/γ-Al_2O_3 and only a small peak in the 2θ= 32°-37° is observed for the conventional sample 5%Co10%Mo/γ-Al_2O_3. This result indicates the trace amount of $CoMoO_4$. These data agree with the elemental analysis of the catalysts. Furthermore, Mn_2O_3, Cr_2O_3, Fe_2O_3, and V_2O_5 (having a relative peak) were confirmed in XRD scan that indicates the presence of crystalline metal oxides, though in a small amount. It is further believed that the species in a material present at concentrations lower than 5%, so they cannot be properly detected by XRD technique. According to the above explanations, very weak peaks of all metals were observed for all the oxide phases.

The N_2-adsorption/desorption results (Table 4) indicated that the surface area of 10%Mo/γ-Al_2O_3 decreased with the loading of other transition metals such as Co, Ni, Mn, Cr, Fe, and V rather than the cases without metals [11]. Catalyst with Co atoms has the largest SA, PV and APD while the one with VMo/ γ-Al_2O_3 has the smallest SA, PV and APD. Fig. 10 reveals the pore size distribution of the sample measured according to BJH method. It can be seen that the catalyst reveals a uniform mesoporous structure. According to the IUPAC classification and Fig. 11, all of the prepared mesopore 10%Mo/γ-Al_2O_3 catalysts exhibited type IV isotherms with H_2 hysteresis loop [11].

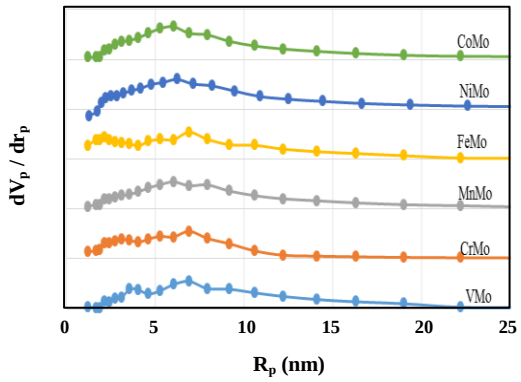

Fig. 10: BJH plot of different transition metals.

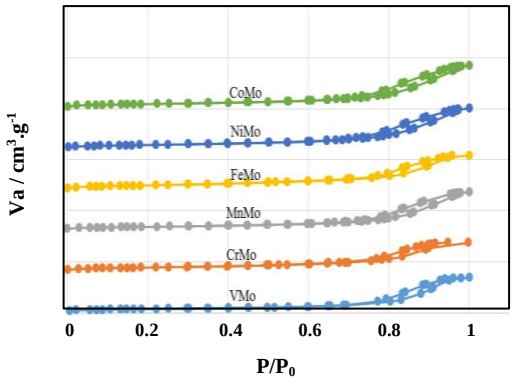

Fig. 11: Adsorption/desorption isotherms of different transition metals.

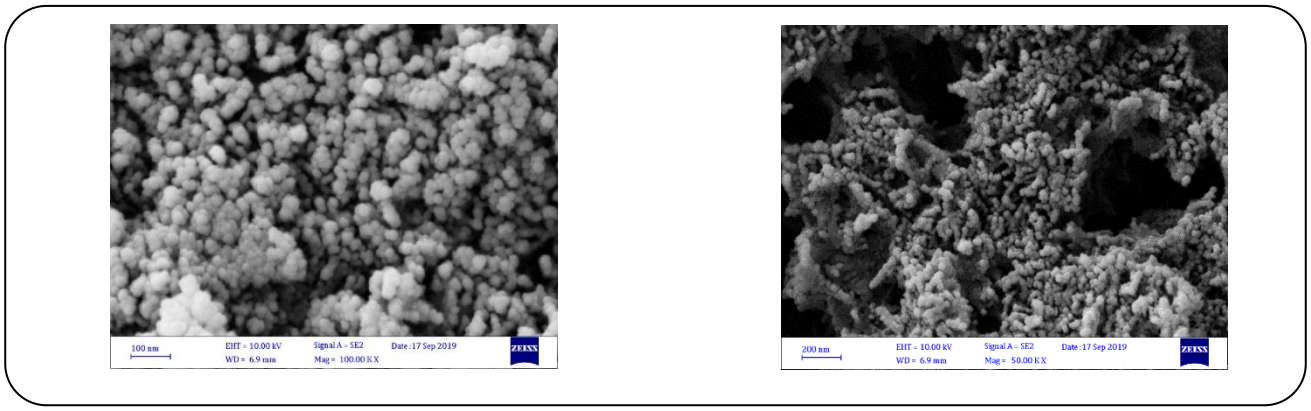

Fig. 12: SEM Images of the 10wt.%Mo/γ- Al_2O_3 (left) and optimum sample **5%Co10%Mo/γ-Al_2O_3** *(right).*

Table 5 shows the results of the ICP-MS analysis of the prepared catalysts with transition metals such as Co, Ni, Mn, Cr, Fe, or V with 10% Mo a pH=4. SEM images (Fig. 12) indicate that no agglomeration of two metals exists (right figure) on the prepared catalyst. It was found that the distribution and impregnation of metals were done well. Hence, a more homogenous impregnation was taken place. Moreover, these two metals lead to the production of a catalyst with uniform particle size distribution. Fig. 13 shows NH_3-TPD profile of the 5%Co10%Mo/γ-Al_2O_3 catalyst. For this catalyst, the spectrum indicated two well-resolved peaks at 420 ˚C and 880 ˚C. The results of this section showed that two types of adsorption sites for NH_3-TPD are present on the catalyst. The peak at the temperature of 880 ˚C is attributed to N_2 and H_2 gases produced from the decomposition of NH_3. The peak at the temperature of 420 ˚C is due to releasing the adsorbed NH_3 from alumina and introducing the strong acidic sites.

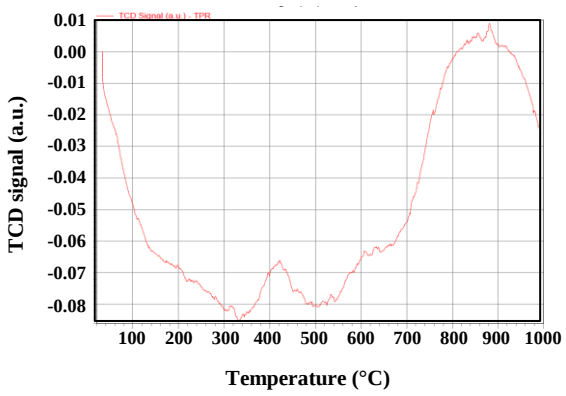

Fig. 13: NH_3-TPD analysis spectrum of the optimum sample (5%Co10%Mo/γ-Al_2O_3).

The kinetics of the reaction

In previous sections, the optimum ODS catalyst (5%Co10%Mo/γ-Al_2O_3) was determined. To test the performance of this catalyst, the kinetics of the oxidative

Table 6: The results of the experiments.

Time (min)	Total sulfur without catalyst	Total sulfur with catalyst
0	160	160
10	145	110
20	138	80
30	133	55
40	123	40
50	118	25
60	114	18
70	111	18
80	105	18
90	105	18
100	105	18
110	105	18
120	105	18

Table 7: The results of the kinetics investigation by affinity model.

	$\lvert A_r/RT \rvert$	t_k (min)
Without catalyst	0.76	159.41
With catalyst	0.87	78.38

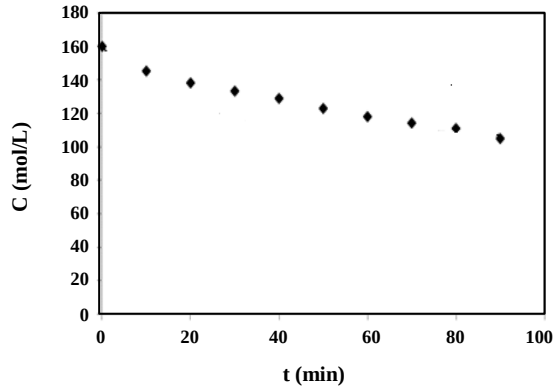

Fig. 14: The variations of sulfur concentration versus time without catalyst.

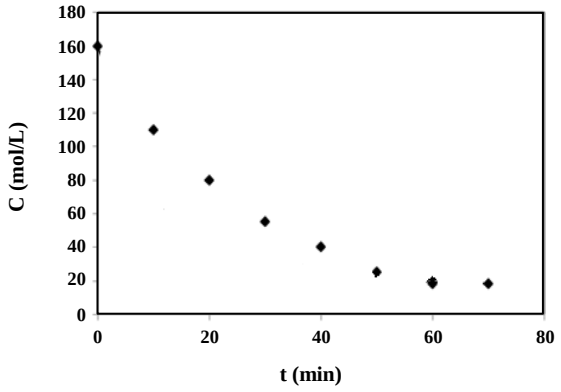

Fig. 15: The variations of sulfur concentration versus time in the presence of 5%Co10%Mo/γ-Al_2O_3 catalyst.

desulfurization was determined with and without the presence of ODS catalyst. The chemical affinity model was used to determine the kinetic parameters of this reaction. This model is simple and it can be used only based on the concentration of the sulfur. Moreover, it does not require heat or mass transfer coefficients. Therefore, among different kinetic models, the chemical affinity model was selected for this study. The results of the model are presented in Tables 6, 7, and Figs. 14-17.

The obtained results show that the presence of the catalyst increases the normalized rate constant and decreases the equilibrium time of the reaction. Therefore, it significantly

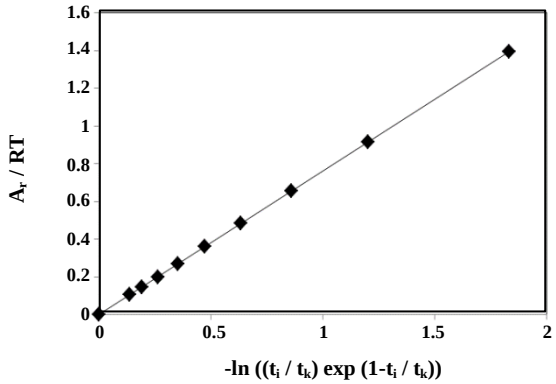

Fig. 16: Affinity variations versus –ln[(ti/tk) exp (1–(ti/tk))] without catalyst.

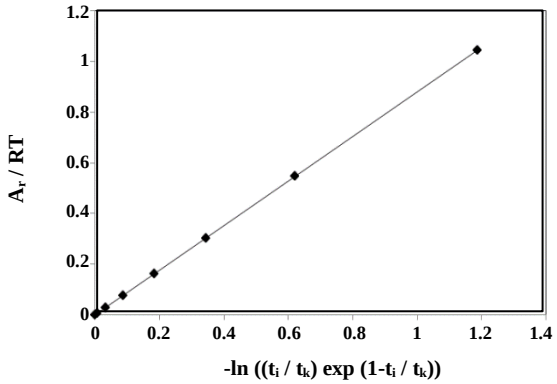

Fig. 17: Affinity variations versus –ln[(ti/tk) exp(1–(ti/tk))] in the presence of 5%Co10%Mo/γ-Al2O3 catalyst.

improves the kinetics of desulfurization reaction. Therefore, it is concluded that the applied catalyst performs well for desulfurization reaction.

CONCLUSIONS

The influence of pH, molybdenum content, and some of the transition metals, including Vanadium, Chromium, Manganese, Iron, Cobalt, and Nickel on the properties of catalyst and performance of oxidative desulfurization (ODS) was determined. The results of this study proved that the oxidative activity of Mo/γ-Al_2O_3 catalyst increased when Mo content increased up to about 10%. It decreased when Mo content was lower than this value. It can be concluded that the optimum condition of alumina catalyst was 10% of molybdenum at pH=4 by using phosphoric acid. The addition of transition metals onto the Mo10%/γ-Al_2O_3 catalysts resulted in a significant increase in the sulfur removal of ODS reaction. Experimental data showed that the catalytic activity of the oxidative desulfurization reaction followed this order: CoMo/γ-Al_2O_3> NiMo/γ-Al_2O_3> FeMo/γ-Al_2O_3> CrMo/γ-Al_2O_3> MnMo/γ-Al_2O_3> VMo/γ-Al_2O_3. Furthermore, the improvement on the molybdenum catalyst indicated that oxidative desulfurization for light naphtha was achieved over the 5% of cobalt calcined at 600ºC. The BET results of 5%Co10%Mo/γ-Al_2O_3 showed that the SA, MPD, and PV have the highest amount in comparison with the other transition metals and led to an increase in sulfur removal. By using this catalyst in the catalytic ODS reactor at 25ºC and ambient pressure, the total sulfur of the light naphtha decreased from 160ppm to 20 ppm. The SEM images showed that the application of Co and Mo metals reaches more homogenous impregnation and indicates that no agglomeration of two metals exists (right figure) on the prepared catalyst. The NH_3-TPD result introduced the strong acidic sites of 5%Co10%Mo/γ-Al_2O_3. The kinetic model based on the chemical affinity showed that the applied catalyst significantly increases the removal rate of sulfur from naphtha. The present method based on using mild operating conditions, low cost of the catalyst, high conversion of the sulfur, and simple mechanization can be considered as forwarding steps of the industrial process of desulfurization for fuel oil. The chemical affinity model is simple, requires only the concentration of sulfur, computing all-important kinetic parameters, and does not require the heat or mass transfer coefficients. The results of the kinetic studies on the optimum sample (5%Co10%Mo/γ-Al_2O_3 catalyst) showed that t_k=78.38 min and [A_r/RT]=0.87.

Acknowledgments

The authors would like to thank Guilan University for their support. The authors would like to acknowledge Mr. Fadavi director of research and technology of the Arak Oil Refining Company and Mrs. Soheila Sheybani for financial support of this project.

Appendix

The Chemical Affinity Model

The chemical affinity model has been applied to several studies. The important aspects of this model are explained. The chemical affinity (A_i) is defined as a generalized

driving force of a chemical reaction. It can be expressed as follows:

$$A_i = -\sum_j (\nu_j \mu_j)_i \quad (1)$$

In the above equation, μ_i is the chemical potential of component *i*.

Using the thermodynamic equation of chemical potential, the following equation is derived for chemical affinity:

$$\nu_j \mu_j = \nu_j \mu_j^o + RT \ln (a_j)^{\nu_j} \quad (2)$$

All experiments are conducted at a constant temperature; therefore, Equation (1) can be stated as follows:

$$A_i = A_i^o - RT \sum_j (\ln (a_j)^{\nu_j})_i \quad (3)$$

In Equation (3), A^o shows the affinity at standard conditions. *A* indicates a temperature-dependent term.

The chemical affinity model considers Q_i as an activity ratio. This parameter is defined as follows:

$$Q_i = \prod_j ((a_j)^{\nu_j})_i \quad (4)$$

Based on Equation (4), Equation (3) is restated as follows:

$$A_i = A_i^o - RT \ln (Q_i) \quad (5)$$

When the system is at the equilibrium condition, A_i=0 and A_i^o=RT ln(*K*). *K* shows the thermodynamic equilibrium constant. Considering Equation (5), the following expression can be derived:

$$A_i = -RT \ln (\zeta_{Q_i}) \quad (6)$$

in which

$$\zeta_{Q_i} = (\frac{Q_i}{K}) \quad (7)$$

When a reaction takes place in a closed system, constant volume, and at a constant temperature, one can calculate the affinity decay rate from the following equation:

$$\mathring{A}_{T,V} = \left(\frac{\partial A_i}{\partial t} \right)_{T,V} \quad (8)$$

The previous studies proved that $\mathring{A}_{T,V}$ inversely depends on time. Therefore, the chemical affinity can be expressed based on Eq. (9):

$$\frac{A_i}{RT} = -\frac{A_r}{RT} \left[-\ln \left(\frac{t_i}{t_k} \exp (1 - \frac{t_i}{t_k}) \right) \right] \quad (9)$$

In the above equation, $\zeta_{t_i} = \left(\frac{t_i}{t_k} \right)$. To reproduce the experimental kinetic data, the value of ζ_{t_i} must be determined so that t_K must be computed. The value of t_k is computed by using the iterative approach.

To compute the parameters of the chemical affinity model, the extent of the sulfur removal in terms of time is determined. Instead of activity, the concentration of sulfur during the sulfur removal reaction has been chosen to determine the extent of the reaction. This extent is defined as follows:

$$\zeta_{Q_i} = \frac{n_{ci}}{n_{cf}} = \frac{n_o - n_i}{n_o - n_f} \quad (10)$$

Where subscripts *o* and *f* are the initial and the equilibrium conditions, respectively.

$$n_o = C_o V \quad (11)$$

$$n_i = C_i V \quad (12)$$

$$n_f = C_f V \quad (13)$$

In Equations (11) and (13), C_o and C_f show the initial and equilibrium concentrations of the sulfur, respectively. To our knowledge, volume and temperature are constant in Equations (11-13).

Combining Equations (10-13, 14) (in a fixed volume and constant temperature) is derived:

$$\zeta_{Qi} = \frac{n_{ci}}{n_{cf}} = \frac{n_o - n_i}{n_o - n_f} = \frac{C_o V - C_i V}{C_o V - C_f V} = \frac{C_o - C_i}{C_o - C_f} \quad (14)$$

When Equation (6) and Equation (14) are combined, the chemical affinity can be written as follows:

$$\frac{A_i}{RT} = -\ln\left(\frac{n_{ci}}{n_{cf}}\right) = -\ln\left(\frac{C_o - C_i}{C_o - C_f}\right) \quad (15)$$

Combining Equations (10) and (16), Equation (16) is stated as follows:

$$\frac{n_{ci}}{n_{cf}} = \frac{C_o - C_i}{C_o - C_f} = \left[\left(\frac{t_i}{t_k}\exp(1-\frac{t_i}{t_k})\right)\right]^{\frac{-A_r}{RT}} \quad (16)$$

t_k and $-A_r/RT$ show the kinetic parameters of the present model. The value of $\left(\left|\frac{A_r}{RT}\right|\right)$ is known as a normalized rate constant of the model. If A_i versus $\ln\left[\zeta_{t_i}.\exp\left(1-\zeta_{t_i}\right)\right]$ is plotted, the values of A_r and t_k can be calculated.

Received : June 13, 2020 ; Accepted : Aug. 3, 2020

REFERENCES

[1] Saleh T. A., Characterization, Determination and Elimination Technologies for Sulfur from Petroleum: Toward Cleaner Fuel and a Safe Environment, *Trends in Environmental Analytical Chemistry*, **25**: e00080 (2020).

[2] Ghorbani N., Moradi G., Oxidative Desulfurization of Model and Real Oil Samples Using Mo Supported on Hierarchical Alumina–Silica: Process Optimization by Box–Behnken Experimental Design, *Chinese Journal of Chemical Engineering*, **27**: 2759-2770 (2019).

[3] Subhan S., Rhman A. U., Yseen A., Rshid H., Ishaq M., Sahibzada M., Tong Z., Ultra-Fast and Highly Efficient Catalytic Oxidative Desulfurization of Dibenzothiophene at Ambient Temperature over Low Mn Loaded Co-Mo/Al_2O_3 and Ni-Mo/Al_2O_3 Catalysts Using NaClO as Oxidant, *Fuel*, **273:** 793-805 (2019).

[4] Yseen A., Rshid H., Subhan S., Rhman A. U., Sahibzada M., Tong Z., Boosting the Hydrodesulfurization of Dibenzothiophene Efficiency of Mn Decorated (Co/Ni)-Mo/Al_2O_3 Catalysts at Mild Temperature and Pressure by Coupling with Phosphonium Based Ionic Liquids, *Chemical Engineering Journal*, **375**: 121957 (2019).

[5] Speight J. G., Introduction of Handbook of Refinery Desulfurization, "Handbook of Refinery Desulfurization", CD & W, Inc. Laramie, Wyoming, (2016).

[6] Garcıa-Gutierrez J. L., Gustavo A. F., Maria Eugenia H., Ponciano G., Florentino M., Federico J., Ultra-Deep Oxidative Desulfurization of Diesel Fuel by the Mo/Al_2O_3-H_2O_2 System: The Effect of System Parameters on Catalytic Activity, *Applied Catalysis A: General*, **334**: 366–373 (2008).

[7] Grilic M., Likozar B., Levec J., Hydrotreatment of Solvolytically Liquefied Lignocellulosic Biomass over NiMo/Al_2O_3 Catalyst: Reaction Mechanism, Hydrodeoxygenation Kinetics and Mass Transfer Model Based on FTIR, *Biomass & Bioenergy*, **63**: 300-312 (2014).

[8] Grilc M., Likozar B., Levec J., Hydrodeoxygenation and Hydrocracking of Solvolysed Lignocellulosic Biomass by Oxide, Reduced And Sulphide form of NiMo, Ni, Mo and Pd Catalysts, *Applied Catalysis B: Environmental*, **275**:150–151(2014).

[9] Grilc M., Veryasov G., Likozar B., Jesih A., Levec J., Hydrodeoxygenation of Solvolysed Lignocellulosic Biomass by Unsupported MoS_2, MoO_2, Mo_2C and WS_2 Catalysts, *Applied Catalysis B: General* **163:** 467-477(2015).

[10] Ancheyta J., "Introduction of Deactivation of Heavy Oil Hydroprocessing Catalyst", *Deactivation of Heavy Oil Hydroprocessing Catalyst*, John Wiley & Sons, Inc., Hoboken, New Jersey, (2016).

[11] Wan Abu Bakar W., Rusmidah A., Abdul Aziz A., Wan MokhtarW., The Role of Molybdenum Oxide Based Catalysts on Oxidative Desulfurization of Diesel Fuel, *Modern Chemistry & Application*, **3:** 1-3 (2015).

[12] Rang H., Kann J., Oja V., Advances in Desulfurization Research of Liquid Fuel, *Oil Shale*, **23:** 164-176 (2008).

[13] Akbari A., Omidkhah M., Toufighi Darian J., Preparation and Characterization of MoO_3/Al_2O_3 Catalyst for Oxidative Desulfurization of Diesel using H_2O_2: Effect of Drying Method and Mo Loading, *International Journal of Chemical and Molecular Engineering*, **6:** 567-570 (2012).

[14] Garcıa-Gutie´rrez J. L., Gustavo A. F., Maria Eugenia H., Florentino M., Juan N., Federico J., Ultra-Deep Oxidative Desulfurization of Diesel Fuel with H_2O_2 Catalyzed under Mild Conditions by Polymolybdates Supported on Al_2O_3, *Applied Catalysis A: General*, **305:** 15–20 (2006).

[15] March J., Reactions, Mechanisms, and Structure, *Advanced Organic Chemistry*, Wiley-Interscience, New York, (1992).

[16] Ramirez L.F., Murrieta F., Garcia-Gutierrez J.L., Saint Martin-Castan R., Martinez-Guerrero M., Montiel-Pacheco M., Mata-Diaz R., Desulfurization of Middle Distillates by Oxidation and Extraction Process, *Pet. Sci. Technol.* **22:** 129-139 (2004).

[17] Te M., Fairbridge C., Ring Z., Oxidation Reactivities of Dibenzothiophenes in Polyoxometalate/H_2O_2 and Formic Acid/H_2O_2 System, Oxidation Reactivities of Dibenzothiophenes in Polyoxometalate/H_2O_2 and Formic Acid/H_2O_2 System, *Appl. Catal. A*, **219**: 267-280 (2001).

[18] Wan Abdullah W., Rusmidah A., Wan Abu Bakar W., Oxidation of Commercial Petronas Diesel with Tert-Butyl Hydroperoxide over Polymolybdate Alumina Supported Catalyst Modified with Alkaline Earth Metals, *Malaysian Journal of Analytical Sciences*, **20:** 296-302 (2016).

[19] Wenwu Zh., Yanan Zh., Xiujuan T., Yasong Zh., Qiang W., Sijia D., Effects of Gallium Addition to Mesoporous Alumina by Impregnation on Dibenzothiophene Hydrodesulfurization Performances of the Corresponding NiMo Supported Catalysts, *Fuel*, **228:** 152–163 (2018).

[20] Yaseen M., Shoukat A., Rahman A., Ur Rashid H., Waqas A., Oxidative Desulfurization of Dibenzothiophene over Fe Promoted Co-Mo/Al_2O_3 and Ni-Mo/Al_2O_3 Catalysts Using Hydrogen Peroxide and Formic Acid as Oxidants, *Chinese Journal of Chemical Engineering*, **26:** 593-600 (2017).

[21] Shahidian Z., Zare K., Moosavi M., Modification of Mesoporous Extrudate Gamma Alumina through Thermal Ammonia Treatment**,** *Iranian Journal of Chemistry and Chemical Engineering (IJCCE)*, **39(3):** 61-69 (2020).

[22] Shahidian Z., Zare K., Moosavi M., Improvement of Heavy Oil Hydrodesulfurization Catalyst Support Properties by Acetic Acid Treatment**,** *Iranian Journal of Chemistry and Chemical Engineering (IJCCE)*, **39(3):** 71-80 (2020).

[23] Morales A., Ramirez de Agudelo M.M., Promoter Role of Octahedral Co (and Ni) in Modified Co(Ni)Mo-Al_2O_3 Catalysts for Hydrodesulfurization Reactions, *Applied Catalysis*, **23:** 23-34 (1986).

[24] Fattahi M., Kazemeini M., Khorasheh F., Rashidi A. M., Morphological Investigations of Nanostructured V_2O_5 over Graphene Used for ODHP Reaction: From Synthesis to Physiochemical Evaluations, *Catalysis Science and Technology*, **5(2):** 910-924 (2015).

[25] Fattahi M., Kazemeini M., Khorasheh F., Rashidi A. M., Kinetic Modeling of Oxidative Dehydrogenation of Propane (ODHP) over a Vanadium-Graphene Catalyst: Application of the DOE and ANN Methodologies, *Journal of Industrial and Engineering Chemistry*, **20:** 2236-2247 (2014).

[26] Fattahi M., Kazemeini M., Khorasheh F., Rashidi A. M., An Investigation of the Oxidative Dehydrogenation of Propane Kinetics over a Vanadium–Graphene Catalyst Aiming at Minimizing of CO_x Species, *Chemical Engineering Journal*, **250:** 14-24 (2014).

[27] Payan A., Fattahi M., Roozbahani B., Synthesis, Characterization and Evaluations of TiO_2 Nanostructures Prepared from Different Titania Precursors for Photocatalytic Degradation of 4-Chlorophenol in Aqueous Solution, *Journal of Environmental Health Science and Engineering*, **16:** 41-54 (2018).

[28] Barghi B., Fattahi M., Khorasheh F., Kinetic Modeling of Propane Dehydrogenation over an Industrial Catalyst in Presence of Oxygenated Compounds, Reaction Kinetics, *Mechanisms and Catalysis Journal*, **107:** 141-155 (2012).

[29] Barghi B., Fattahi M., Khorasheh F., The Modeling of Kinetics and Catalyst Deactivation in Propane Dehydrogenation Over Pt-Sn/γ-Al_2O_3 in Presence of Water as an Oxygenated Additive, *Petroleum Science and Technology*, **32:** 1139-1149 (2014).

[30] Garfinkle M., The Thermodynamic Natural Path in Chemical Reaction Kinetics, *Discrete Dynamics in Nature and Society*, **4:** 145-164 (2000).

[31] Roosta H., Khosharay S., Varaminian F., Experimental and Modeling Investigation on Mixed Carbon Dioxide–Tetrahydrofuran Hydrate Formation Kinetics in Isothermal and Isochoric Systems, *Journal of Molecular Liquids*, **211:** 411-416 (2015).

[32] Roosta H., Khosharay S., Varaminian F., Experimental Study of Methane Hydrate Formation Kinetics with or without Additives and Modeling Based on Chemical Affinity, *Energy Conversion and Management*, **76:** 499-505 (2013).

[33] Mazraeno M.S., Varaminian, F., Vafaie Sefti, M., Experimental and Modeling Investigation on Structure H Hydrate Formation Kinetics, *Energy Conversion and Management*, **76:** 1-7 (2013).

[34] Naeiji, P., Arjomandi, A., Varaminian, F., Amino Acids as Kinetic Inhibitors for Tetrahydrofuran Hydrate Formation: Experimental Study and Kinetic Modeling, *Journal of Natural Gas Science and Engineering*, **21:** 64-70 (2014).

[35] Hocevar B., Grilc M., Hus M., Likozar B., Mechanism, ab initio Calculations and Microkinetics of Straight-Chain Alcohol, Ether, Ester, Aldehyde and Carboxylic Acid Hydrodeoxygenation over Ni-Mo catalyst, *Chemical Engineering Journal*, **359**: 1339-1351 (2019).

[36] S. Imamura S., Sasaki H., Shono M., Kanaiy H., Structure of Molybdenum Supported on γ, α, and κ- Aluminas in Relation to Its Epoxidation Activity, *Journal of Catalysis*, **177:** 72–81 (1998).

[37] Escobar J., Barrer M., Gutierrez A., Cortes-Jacome M., Angeles-Chavez A., Toledo J., Solis-Casados D., Highly Active P-doped Sulfided NiMo/Alumina HDS Catalysts from Mo-blue by Using Saccharose as Reducing Agents Precursor, *Applied Catalysis B: Environmental*, **237:** 708–720 (2018).

[38] Gutierrez J., Fuentes A., Hernandez-Teran M., Murrieta F., Navarrete J., Jimenez-Cruz F., Ultra-Deep Oxidative Desulfurization of Diesel Fuel with H_2O_2 Catalyzed under Mild Conditions by Polymolybdates Supported on Al_2O_3, *Applied Catalysis A: General*, **305:** 15–20 (2006).

[39] Hamiye R., Lancelot C., Blanchard P., Toufaily J., Hamieh T., Lamonier C., Diesel HDS Performance of Alumina Supported CoMoP Catalysts Modified by Sulfone Molecules Produced by ODS Process, *Fuel*, **210:** 666–673 (2017).

[40] Bouwens S., Van Der Kraan A., De Beer V., Prins R., The Influence of Phosphorus on the Structure and Hydrodesulfurization Activity of Sulfided Co and Co-Mo Catalysts Supported on Carbon and Alumina, *Journal of Catalysis*, **128:** 559-568 (1991).

[41] Bergwerff J.A., Van de Water L.G.A., Visser T., Peinder P., Leliveld B. R.G., Jong K.P., Weckhuysen B.M., Spatially Resolved Raman and UV-Visible-NIR Spectroscopy on the Preparation of Supported Catalyst Bodies: Controlling the Formation of $H_2PMo11CoO40$-5 Inside Al_2O_3 Pellets During Impregnation, *Chem. Eur. J.*, **11:** 4591 – 4601 (2005).

[42] Choi J., Yoo K. S., Kim S. D., Park H. K., Chul-Woo Nam C. W., Jinsoo Kim J., Synthesis of Mesoporous Spherical g-Al_2O3 Particles with Varying Porosity by Spray Pyrolysis of Commercial Boehmite, *Journal of Industrial and Engineering Chemistry*, **56:** 151-156 (2017).

[43] Parkhomchuk E. V., Lysikov A. I., Okunev A. G., Parunin P. D., Semeikina V. S., Ayupov A. B., Trunova V. A., Parmon V. N., Meso/Macroporous CoMo Alumina Pellets for Hydrotreating of Heavy Oil, *Industrial and Engineering Chemistry Research*, **52:** 17117-17125 (2013).

[44] Ferdous D., Dalai A. K., Adjaye J., A series of $NiMo/Al_2O_3$ Catalysts Containing Boron and Phosphorus Part I. Synthesis and Characterization, *Applied Catalysis A: General*, **260:** 137–151 (2004).

[45] Liu F., Xu S., Cao L., Chi Y., Zhang T., Xue D., A Comparison of $NiMo/Al_2O_3$ Catalysts Prepared by Impregnation and Coprecipitation Methods for Hydrodesulfurization of Dibenzothiophene, *J. Phys. Chem. C.*, 111: 7396-7402 (2007).

[46] Hassani H., Batol Zakerinasab B., Hossien Poor H., Synthesis, Characterization and Application of Alumina/ Vanadium Pentoxide Nanocomposit by Sol-Gel Method, *Applied Organometallic Chemistry*, **3945:** 1-7 (2017).

[47] Wang X.J., Li H.D., Fei Y.J., Wang X., Xiong Y.Y., Nie Y.X., Feng K.A., XRD and Raman Study of Vanadium Oxide Thin Films Deposited on Fused Silica Substrates by RF Magnetron Sputtering, *Applied Surface Science*, **177**: 8-11 (2001).

[48] Ketseng T., Hsinchu H., Characterization of ç-Alumina-Supported Manganese Oxide as an Incineration Catalyst for Trichloroethylene, *Environ. Sci. Technol.*, **37**: 171-176 (2003).

[49] Anandhi J. T., Rayer S. L., T. Chithambarathanu T., Synthesis, FTIR Studies and Optical Properties of Aluminium Doped Chromium Oxide Nanoparticles by Microwave Irradiation at Different Concentrations, *Chemical and Materials Engineering*, **5(2)**: 43-54 (2017).

[50] Kortov V., Kiryakov A., Pustovarov V., Luminescent Properties of Alumina Ceramics Doped with Chro-Mium Oxide, *Journal of Physics: Conference Series*, **741**: 1-5 (2016).